Molecular Vision 2015; 21:273-284 <http://www.molvis.org/molvis/v21/273>
Received 19 March 2013 | Accepted 11 March 2015 | Published 13 March 2015

Presence of *rd8* mutation does not alter the ocular phenotype of late-onset retinal degeneration mouse model

Bhubanananda Sahu,[1] Venkata R.M. Chavali,[1] Akhila Alapati,[1] John Suk,[1] Dirk-Uwe Bartsch,[1] Monica M. Jablonski,[2] Radha Ayyagari[1]

[1]Shiley Eye Institute, University of California San Diego, La Jolla, CA; [2]Hamilton Eye Institute, University of Tennessee Health Science Center, Memphis, TN

Purpose: A spontaneous frameshift mutation, c.3481delC, in the *Crb1* gene is the underlying cause of dysplasia and retinal degeneration in *rd8* mice. The *rd8* mutation is found in C57BL/6N but not in C57BL/6J mouse sub-strains. The development of ocular pathology in single knockout *Ccl2*$^{-/-}$, *Cx3cr1*$^{-/-}$ and in double knockout *Ccl2*$^{-/-}$/*Cx3cr1*$^{-/-}$ mice raised on a C57BL/6 background has been reported to depend on the presence of a *rd8* mutation. In this study, we investigated the influence of the *rd8* mutation on the retinal pathology that we previously described in the late-onset retinal degeneration (L-ORD) mouse model with a heterozygous S163R mutation in the *C1q-tumor necrosis factor-related protein-5* (*Ctrp5*$^{+/-}$) *gene* that was generated on a C57BL/6J background.

Methods: Mouse lines carrying the *Ctrp5* S163R and *rd8* mutations (*Ctrp5*$^{+/-;rd8/rd8}$), corresponding controls without the *rd8* mutation (*Ctrp5*$^{+/-;wt/wt}$), and wild-type mice with and without the *rd8* mutation (*Wt*$^{rd8/rd8}$ and *Wt*$^{wt/wt}$, respectively) were generated by systematic breeding of mice in our L-ORD mouse colony. Genotyping the mice for the *rd8* (del C at nt3481 in *Crb1)* and *Ctrp5* S163R mutations was performed with allelic PCR or sequencing. Retinal morphology was studied with fundus imaging, histology, light microscopy, electron microscopy, and immunohistochemistry.

Results: Genotype analysis of the mice in L-ORD mouse colony detected the *rd8* mutation in the homozygous and heterozygous state. Fundus imaging of wild-type mice without the *rd8* mutation (*Wt*$^{wt/wt}$) revealed no autofluorescence (AF) spots up to 6–8 months and few AF spots at 21months. However, the accumulation of AF lesions accelerated with age in the *Ctrp5*$^{+/-}$ mice that lack the *rd8* mutation (*Ctrp5*$^{+/-;wt/wt}$). The number of AF lesions was significantly increased ($p<0.001$), and they were small and uniformly distributed throughout the retina in the 21-month-old *Ctrp5*$^{+/-;wt/wt}$ mice when compared to the age-matched controls. Wild-type and *Ctrp5*$^{+/-}$ mice with the *rd8* mutation (*Wt*$^{rd8/rd8}$ and *Ctrp5*$^{+/-;rd8/rd8}$, respectively) revealed an integrated retinal architecture with well-defined outer segments/inner segments (OS/IS), outer nuclear layer (ONL), outer plexiform layer (OPL), and inner nuclear layer (INL). The presence of pseudorosette structures reported in the *rd8* mice between the ONL and the INL in the ventral quadrant of the retina was not observed in all genotypes studied. Further, the external limiting membrane was continuous in the *Ctrp5*$^{+/-;rd8/rd8}$ and *Wt*$^{rd8/rd8}$ mice. Evaluation of the retinal phenotype revealed that the *Ctrp5*$^{+/-;wt/wt}$ mice developed characteristic L-ORD pathology including age-dependent accumulation of AF spots, development of sub-retinal, sub-RPE, and basal laminar deposits, and Bruch's membrane abnormalities at older age, while these changes were not observed in the age-matched littermate *WT*$^{wt/wt}$ mice.

Conclusions: The *Wt*$^{rd8/rd8}$ and *Ctrp5*$^{+/-;rd8/rd8}$ mice raised on C57BL/6J did not develop early onset retinal changes that are characteristic of the *rd8* phenotype, supporting the hypothesis that manifestation of *rd8*-associated pathology depends on the genetic background. The retinal pathology observed in mice with the *Ctrp5*$^{+/-;wt/wt}$ genotype is consistent with the L-ORD phenotype observed in patients and with the phenotype we described previously. The lack of *rd8*-associated retinal pathology in the *Ctrp5*$^{+/-;wt/wt}$ mouse model raised on the C57BL/6J background and the development of the L-ORD phenotype in these mice in the presence and absence of the *rd8* mutation suggests that the pathology observed in the *Ctrp5*$^{+/-;wt/wt}$ mice is primarily associated with the S163R mutation in the *Ctrp5* gene.

The Crb complex, first identified in *Drosophila*, is required for polarity and adhesion in embryonic epithelia, stalk membrane morphogenesis in photoreceptors and for the formation of adherens junctions between cells in the retina [1-3]. In mice and humans, the Crb complex is involved in retinal integration and organization [4,5].

The human *crumbs homolog 1* (*CRB1*; Gene ID: 23418, OMIM: 604210) gene encodes a protein containing a signal peptide, 19 epidermal growth-factor (EGF) domains, three A-globular-like domains, and a transmembrane domain [6]. CRB1 is part of the protein complex at adhesion junctions (AJ) and localized to the external limiting membrane (ELM) in the retina. Mutations in the *CRB1* gene are associated with phenotypically diverse retinal disorders including Leber

Correspondence to: Radha Ayyagari, 9415 Campus Point Drive, Shiley Eye Institute, University of California San Diego, La Jolla, CA 92093; Phone: (858) 534-9029; FAX: (858) 246-0568; email: rayyagari@ucsd.edu
Dr. Chavali is now at 133 Anatomy-Chemistry Building, Department of Ophthalmology, University of Pennsylvania, PA, 19104.

congenital amaurosis (LCA), early onset retinitis pigmentosa (e.g., RP12), retinitis pigmentosa with coats-like exudative vasculopathy, and pigmented paravenous retinochoroidal atrophy [7-13]. Four percent of patients with autosomal recessive retinitis pigmentosa (arRP) and 10–15% of patients with autosomal recessive Leber congenital amaurosis (arLCA) carry mutations in the *CRB1* gene [9-11]. The phenotypic diversity of the patients who carry *CRB1* mutations has led to the hypothesis that environmental and genetic modifiers influence the severity and presentation of *CRB1*-associated retinal degeneration [11,14,15].

The naturally occurring *retinal degeneration 8* (*rd8*) mouse model carries a homozygous single base deletion (c.3481delC) in *Crb1* (*Crb1*$^{rd8/rd8}$) causing early onset retinal degeneration, retinal folds, pseudorosettes, focal retinal dysplasia, and ocular spots [5]. The ocular spots correspond to the retinal folds and pseudorosettes that form due to abnormality in the adherens junctions between the photoreceptors and the Müller glia (MG) cells. The outer nuclear layer (ONL) and the inner nuclear layer (INL) are affected in *rd8* mice. The deletion causes a frameshift resulting in a truncated Crb1 protein that consists of only the N-terminal extracellular domain [16].

Similar to patients carrying *CRB1* mutations, phenotypic variations are observed between and within mice strains homozygous for the *rd8* mutation [17]. It has also been reported that the C57BL/6 lines provided by several commercial vendors harbor the *rd8* mutation and present the characteristic *Crb1-a*ssociated phenotype [17]. Although *rd8* mice of the naturally occurring strain (*Crb1*$^{rd8/rd8}$) exhibit ocular spots in the inferior nasal quadrant, the eyes of mice with the *rd8* mutation on the CAST/EiJ background (*CAST/EiJ*$^{rd8/rd8}$) are reported to have fewer spots than the naturally occurring strain [5]. About 19% of the *CAST/EiJ*$^{rd8/rd8}$ mice do not develop ocular spots. Furthermore, N7 generation of *Crb1*$^{rd8/rd8}$ backcrossed with C57BL/6J did not develop retinal spots [5]. The retinal histology of the C57BL/6J mice homozygous for the *rd8* mutation are normal, lacking retinal folds and photoreceptor inner segment (IS) disorganization suggesting that the C57BL/6J background is a strong modulator of the *rd8* phenotype. In contrast, C57BL/6N, a sub-strain derived from C57BL/6J after 1951, harbors the *rd8* mutation and invariably expresses the characteristic *Crb1*-associated phenotype [17]. The discrepancies in the *rd8* phenotype between and within mouse strains provide clear evidence that genetic modifiers influence the development of *rd8* pathology. Two genetically related homozygous *rd8* mouse lines obtained from a backcross with *C57BL/6JOlaHsd* mice display variable phenotypes, and a genetic factor on chromosome 15 has been suggested to be responsible for this variation [18].

The early onset ocular phenotypes observed in HLA-A29 transgenic mice and *CCDKO* mice are associated with presence of the *rd8* mutation and are not due to mutations in the HLA-A29, *Ccl2*, or *Cx3cr1* gene [17]. HLA-A29 transgenic and *CCDKO* mice carrying the *rd8* mutation in the homozygous state exhibit retinal dysplasia. Interestingly, about 20–25% of the HLA-A29 transgenic mice with the *rd8* mutation in the heterozygous state also develop dysplasia [17,19]. The genetic background of the *rd8* mutation differentially modulates the retinal phenotype in the original *CCDKO* and the rederived *Ccl2*$^{-/-}$, *Cx3cr1*$^{-/-}$, and *Ccl2*$^{-/-}$/*Cx3cr1*$^{-/-}$ double-knockout mice. The early onset retinal degeneration seen in *Ccl2*$^{-/-}$/*Cx3cr1*$^{-/-}$ double-knockout mice are dependent on the *rd8* mutation, rather than the synergistic effect of both mutations [19].

We previously reported the ocular phenotype of a knock-in mouse model for late-onset retinal degeneration (L-ORD) caused due to a heterozygous S163R mutation in the *Ctrp5* gene [20]. These mice develop a late-onset retinal degeneration phenotype resembling the clinical phenotype observed in patients with L-ORD, including slower rod b-wave recovery, RPE abnormalities, drusen, Bruch's membrane abnormalities including basal laminar deposits, predominant cone photoreceptor loss with onset around age 13 months, followed by rapid progression of retinal degeneration to near complete loss of cones by 21 months, and an age-dependent accumulation of hyperfluorescent spots [21-23]. Because the L-ORD mouse model (with *Ctrp5*$^{+/-}$ genotype) was developed using embryonic stem (ES) cells from mixed C57BL/6J and C57BL/6N strains and maintained on a C57BL/6J background, we investigated if the rd8 mutation is present in our colonies and whether it influenced the retinal phenotype associated with the *Ctrp5* S163R mutation. The L-ORD mouse model (*Ctrp5*$^{+/-;rd8/rd8}$ *and Ctrp5*$^{+/-;\ wt/wt}$) and the wild-type littermate controls (*Wt* $^{rd8/rd8}$ and *Wt* $^{wt/wt}$) were evaluated for the presence of the *rd8* mutation and its associated phenotype.

METHODS

Animals: The L-ORD mice were generated using ES cells derived from mixed C57BL/6J and C57BL/6N strain background mice [20]. These mouse lines were expanded by crossing with the C57BL/6J strain obtained from Jackson Laboratories (Bar Harbor, ME) to maintain the line. Mice with the desired genotype were generated for the current study by selectively breeding the mice in our L-ORD mice colony to generate the required genotypes. All studies were performed using L-ORD mice and wild-type (WT) littermate

Table 1. PCR primer for genotyping $Wt^{wt/wt}$,$Wt^{rd8/rd8}$, $Ctrp5^{+/-,rd8/rd8}$ mice and for amplification of *rd8* locus for sequencing.

Gene	Allele	Primer name	Sequence (5′-3′)
Crb1	Wild-type	3663-mCrb1 mF1	GTGAAGACAGCTACAGTTCTGATC
		3665-mCrb1 mR	GCCCCATTTGCACACTGATGAC
Crb1	Mutant	3664-mCrb1 mF2	GCCCCTGTTTGCATGGAGGAAACT
			TGGAAGACAGCTACAGTTCTTCTG
		3665-mCrb1 mR	GCCCCATTTGCACACTGATGAC
Crb1	rd8	3666-Crb-F	GGTGACCAATCTGTTGACAATCC
		3667-Crb-R	GCCCCATTTGCACACTGATGAC
Ctrp5	Knock-in	2855-Ctrp5-F	CCCCTACCTTTCGACCGT
		2856-Ctrp5-R	GAAGAAAGAGGCGATGGACTG

mice of age groups 6–8, 9–11, 12–14, and 20–21 months. Five mice of each group were used for autofluorescent-scanning laser ophthalmoscopy (AF-SLO) imaging analyses; three to five mice were used for light microscopy and immunohistochemistry (as described below in the Funduscopy section). All mice were maintained according to the ARVO Statement for the Use of Animals in Ophthalmic and Vision Research and with protocols approved by UCSD Institutional Animal Care and Use Committee.

Detection of the rd8 mutation with allele-specific PCR and sequencing: The mice were genotyped, as described previously [17,20]. Mouse tail DNA was isolated with Qiagen reagents following the manufacturer's instructions (Gentra Puregene Mouse Tail Kit, Qiagen, Valencia, CA). Genotyping and sequencing for the *Crb1* c.3481delC and *Ctrp5* S163R mutations were performed using the primers described in Table 1.

The allele-specific PCR was performed using m*Crb1*mF1, m*Crb1*mF2, and m*Crb1*mR primers as described earlier [5]. The PCR reaction was carried out in a 20 µl reaction volume containing 1.5 mM $MgCl_2$, 100 µM of each dNTP, 1.6 µM each of forward and reverse primer for Wt allele and 0.8 µM of forward and 1.6 µM of reverse primer for rd8 mutate allele with 0.026U AmpliTaq DNA polymerase. Approximately 25 ng of DNA was taken for the reaction. The PCR reaction was initially denatured at 94 °C for 5 min followed by 35 cycles at 94 °C for 30 s, 56 °C for 30 s, 72 °C for 30 s with a final extension of 72 °C for 7 min. Amplification of the wild-type allele produces a 220 bp fragment, and the mutant allele produces a 240 bp fragment. Confirmation of the *rd8* mutation was performed by sequencing the amplicons [17]. Genotyping for the *Ctrp5* S163R knock-in mutation was performed as described earlier [20].

Fundoscopy: Fundoscopy and autofluorescence (AF) imaging were performed using a SPECTRALIS high-resolution, using a SPECTRALIS high-resolution, combination scanning laser ophthalmoscope and spectral domain optical coherence tomography (HRA+OCT) imaging system (Heidelberg Engineering, Inc., Carlsbad, CA) as previously described [20,24-26]. The number of AF spots per eye was counted, and the average number of AF spots per fundus in each group were calculated.

Retinal histology: L-ORD (n=5) and WT (n=5) mice with and without the *rd8* mutation were enucleated and the eyes fixed with the immersion fixation method using 2% paraformaldehyde and 2% glutaraldehyde in 0.1 M phosphate buffer. Eyecups were postfixed in osmium-tannic acid-paraphenylenediamine to preserve neutral lipids [27] before being embedded in Epon 812 per our published methods [28]. Thin sections were examined on a JEM 1200EX II electron (JOEL USA, Inc. Peabody, MA) microscope. Additional eyecups were embedded in methacrylate [17]. Sections (8–10 µm) were stained with hematoxylin and eosin and examined under a light microscope at 20X magnification. Retina cryosections (8–10 µm), obtained from the eyes fixed in 2% paraformaldehyde, were stained for β-catenin using specific antibodies and images were captured with an Olympus FV1000 confocal microscope.

Antibodies: S-opsin antibodies, goat polyclonal (1:200 Chemicon, Temecula, CA), and M-opsin antibody rabbit polyclonal (1:200, Chemicon) were obtained from a commercial source. The anti-mouse secondary antibody conjugated to Alexa fluor 555 and Alexa fluor 488 (1:1,000, Life Technologies, Grand Island, NY) were used to detect the protein expression with immunohistochemistry. β-catenin antibody (1:200; Santa Cruz Biotechnology Inc., Santa Cruz, CA) was used to check the integrity of the external limiting membrane (ELM).

Statistical analysis: Statistical significance between the number of AF spots in the mutant and wild-type mice was determined using the two-tailed, independent Student *t* test.

RESULTS

Detection of the rd8 mutation in L-ORD and WT mice: Analysis of mice in the L-ORD mouse model colony revealed the presence of the *rd8* mutation. The location and identity of the mutation were confirmed with dideoxy sequencing (Figure 1A). In the L-ORD mouse model colony, the *rd8* mutation

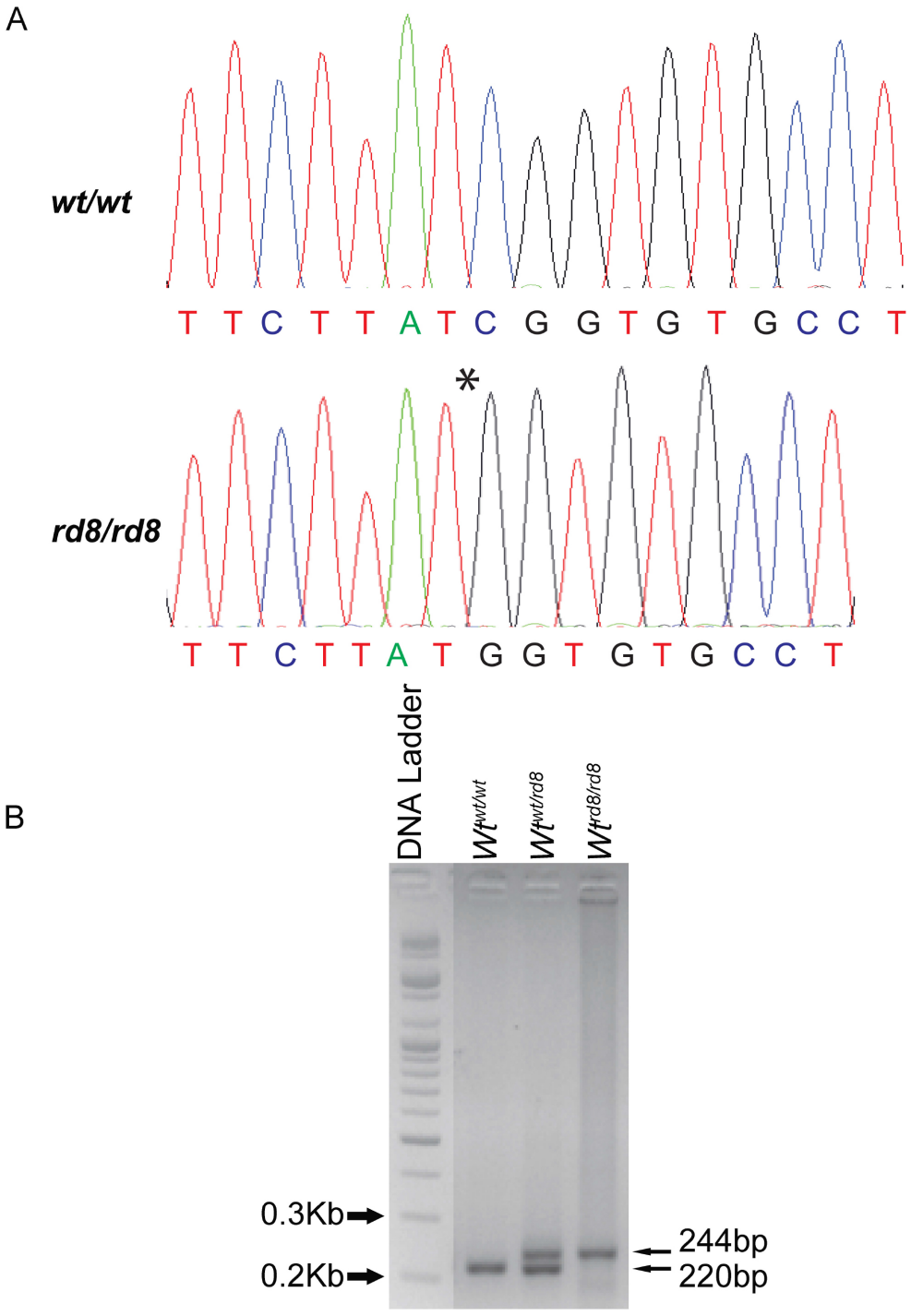

Figure 1. Detection of the *rd8* mutation with sequencing and agarose gel analysis. **A**: Sequence of the *Crb1* locus showing the wild-type and the c.3481delC mutant allele in the homozygous state. The asterisk denotes the deletion. **B**: Agarose gel electrophoresis showing the migration of PCR amplicons for the *rd8* locus from *Wt* mice (220 bp), mice heterozygous (244 bp and 220 bp) and homozygous (244 bp) for the *rd8* mutation. The DNA ladder was included to indicate the size of amplicons. $Wt^{wt/wt}$, *Crb1* wild-type; $Wt^{wt/rd8}$, heterozygous for the *Crb1* mutation; $Wt^{rd8/rd8}$, homozygous for the *Crb1* mutation.

was detected in the L-ORD mice and the WT littermate controls (Figure 1B). The majority of the mice carried the *rd8* mutation in the homozygous or heterozygous state, while a minor proportion were negative for the *rd8* mutation.

Ocular phenotype of L-ORD (Ctrp5$^{+/-;wt/wt}$) and WT littermate control (*Wt*$^{wt/wt}$) mice: The presence of ocular spots is a common finding in L-ORD and *rd8* mice strains. AF-SLO was used to document the ocular phenotype of *Ctrp5*$^{+/-;wt/wt}$ mice (n=5) and age-matched littermates *Wt*$^{wt/wt}$ (n=5; Figure 2). Autofluorescent spots were not observed in the 6- to 8-month-old and 9- to 11-month-old *WT*$^{wt/wt}$ mice (0±0). Few spots were visualized in the 12- to 14-month-old and 20- to 21-month-old *WT*$^{wt/wt}$ mice (23±7 and 70±26, respectively). In contrast, the *Ctrp5*$^{+/-;wt/wt}$ mice displayed more spots by 12–14 months (116±72). The accumulation of AF spots in the *Ctrp5*$^{+/-;wt/wt}$ mice was accelerated with age and increased several fold by 20–21 months (1569±105). The AF spots were small and round and distributed evenly throughout the retina in the *Ctrp5*$^{+/-;wt/wt}$ mice.

Retinal morphology of Ctrp5$^{+/-;wt/wt}$*, Wt*$^{wt/wt}$*, and Wt*$^{rd8/rd8}$ mice: Retinal morphology was studied to evaluate the integrity of the retinal tissue. The gross retinal morphology of the *Wt*$^{rd8/rd8}$ mice was compared with the *Wt*$^{wt/wt}$ mice in our L-ORD mouse colony (Figure 3). Both sets of wild-type mice showed normal retinal morphology and lacked the changes associated with the *rd8* genotype at 8 months of age. The INL, ONL, outer plexiform layer (OPL), and outer segments (OS) were normal in these mice. In addition, pseudorosette structures in the OPL and sub-retinal space that are prominent characteristic features of the *rd8* phenotype were absent in all mice.

The retinal architecture of the *Ctrp5*$^{+/-;wt/wt}$ mice was studied up to 21 months and compared with the phenotype of the age-matched *Wt*$^{wt/wt}$ littermate control mice (Figure 4). Under light microscopy, these mice did not show significant morphological changes including the abnormalities typically associated with the *rd8* phenotype.

Ultrastructural analysis of the RPE was performed on *Ctrp5*$^{+/-;wt/wt}$ mice (n=3) at 9, 14, and 21 months. The *Wt*$^{wt/wt}$ mice (n=3) aged 21 months were used as a control to compare the pathology (Figure 5). The *Wt*$^{wt/wt}$ mice had normal RPE with well-organized basal infoldings and an intact Bruch's membrane. RPE abnormalities were prominent as early as 9 months in the *Ctrp5*$^{+/-;wt/wt}$ mice. The RPE basal infoldings were disorganized and displaced from Bruch's membrane. Numerous vacuoles and phagolysosomes were found throughout the cytoplasm, and several packets of undigested membranous debris were found in the basal RPE. Focal basal laminar deposits and basal linear deposits were found in Bruch's membrane by 14 months. The same abnormalities were also found in the 21-month-old *Ctrp5*$^{+/-;wt/wt}$ mice.

External limiting membrane is continuous in Ctrp5$^{+/-;\ rd8/rd8}$ mouse: To determine whether the loss of *Crb1* affects ELM integrity, we studied the localization of β-catenin in the *Ctrp5*$^{+/-;wt/wt}$ and *Ctrp5*$^{+/-;rd8/rd8}$ mice and compared its localization with the *Wt*$^{wt/wt}$ mouse retina. The anti-β-catenin antibody strongly stained the ELM in all mice including those with the *rd8* mutation (Figure 6), and the pattern of staining indicated the presence of continuous ELM not only in the *Wt*$^{wt/wt}$ mice but also in the mice that had the *rd8* mutation. These results demonstrate the presence of a continuous ELM.

Analysis of previously published Ctrp5$^{+/-}$ mice and WT controls for the rd8 genotype and phenotype: Systematic analysis of the *Ctrp5*$^{+/-}$ mice and their littermate controls was previously described by Chavali et al. [20]. Recent analysis of the tail DNA of the mice reported in Chavali et al. [20] for the *Crb1* mutation revealed that the WT and *Ctrp5*$^{+/-}$ mice presented in that study had the *rd8* genotype either in the heterozygous or homozygous state (Table 2). A review of retinal morphology of these mice presented in that publication revealed a lack of the characteristic features of *rd8* pathology in the *Ctrp5*$^{+/-}$ mice and the WT littermate controls up to 21 months [20]. Specifically, pseudorosettes were absent, and morphological changes suggestive of abnormal ELM were not observed. Ultrastructure analysis showed no abnormalities in the retina of the littermate control mice carrying the *rd8* mutation up to 21 months (Table 2) [20]. The retinal ultrastructure of the *Ctrp5*$^{+/-}$ mice also had no apparent pathology until 5 months of age. However, in mice older than 12 months, the IS of the rods and cones were mildly swollen.

DISCUSSION

Analysis of our L-ORD mouse colony on a C57BL/6J background revealed the presence of the *rd8* mutation [20]. In contrast to the findings reported in the original *rd8* strain [5], *Wt*$^{wt/wt}$, *Wt*$^{rd8/rd8}$, and *Ctrp5*$^{+/-;\ rd8/rd8}$ mice in our L-ORD mouse colony failed to exhibit the abnormal ocular pathology associated with the *rd8* mutation up to 21 months of age, the longest time point presented in this study. In addition, the *Ctrp5*$^{+/-}$ mice free of the *rd8* mutation developed the characteristic L-ORD-associated pathology.

The *rd8* mice were reported to develop AF lesions that were detected as early as 3 weeks of age [5]. These lesions were large, irregular, and heavily concentrated in the inferior nasal quadrant of the fundus. Clinically, these lesions correspond to the region with retinal folds and pseudorosettes that involve the photoreceptors [29]. The laminar folds and pseudorosettes in *rd8* mice were visualized between the ONL

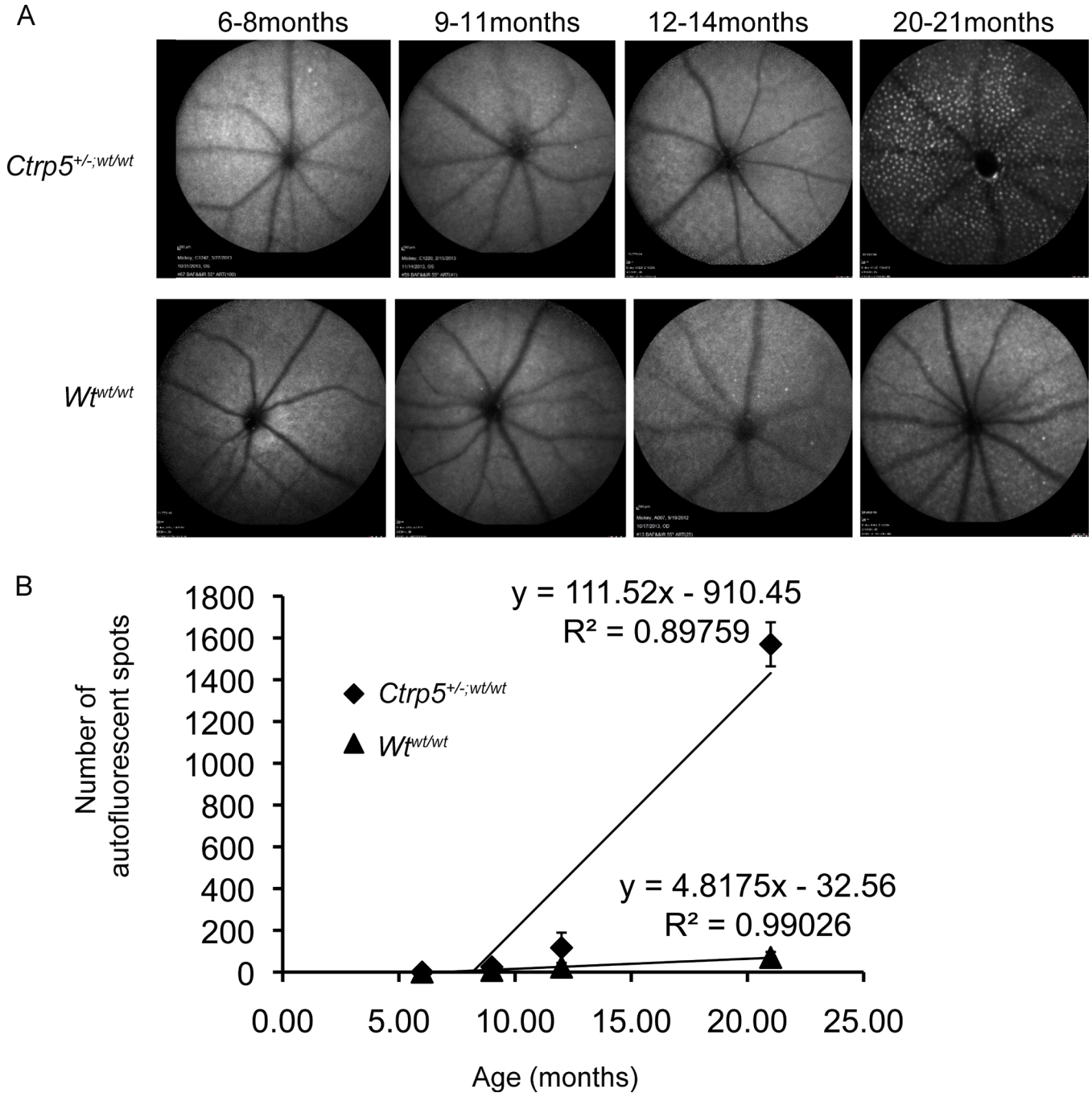

Figure 2. Autofluorescence SLO fundus images of L-ORD mice lacking the *rd8* mutation. **A**: Representative autofluorescent-scanning laser ophthalmoscopy (AF-SLO) images of C57BL/6 wild-type control mice free of the *rd8* mutation ($Wt^{wt/wt}$) and late-onset retinal degeneration (L-ORD) mice free of the *rd8* mutation ($Ctrp5^{+/-;wt/wt}$). The $Wt^{wt/wt}$ mice showed few AF spots by 21 months. However, the AF spots were significantly increased in the $Ctrp5^{+/-;wt/wt}$ mice by 21 months of age. Magnification bar=200 µm. **B**: Quantification of the AF spots in $Wt^{wt/wt}$ (black triangle) and $Ctrp5^{+/-;wt/wt}$ (black diamond) per the AF-SLO images. The number of AF spots is shown as the mean number of spots ± SD. There was an age-related increase in AF spots (linear regression plot) in both genotypes. However, the AF spots accumulated to a high number in L-ORD mice by 21 months when compared to the age-matched control mice ($p<0.001$).

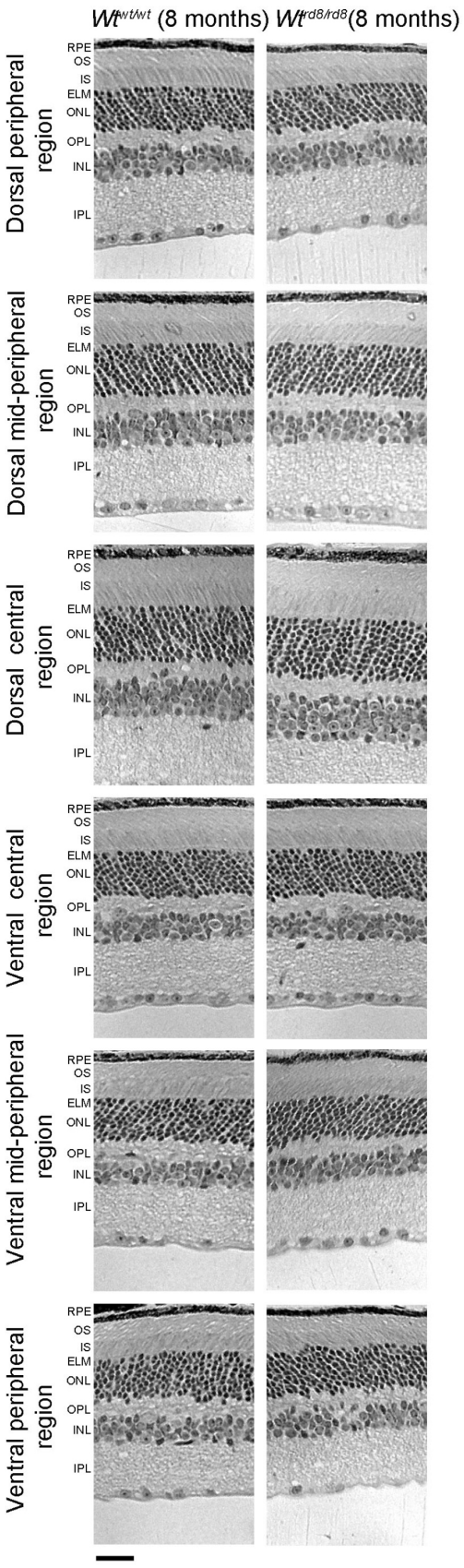

Figure 3. Histological analysis of the retina structure of 8-month-old $Wt^{wt/wt}$ and $Wt^{rd8/rd8}$ mice. The retinas from 8-month-old $Wt^{wt/wt}$ and $Wt^{rd8/rd8}$ mice showed no dysplasia. mo, month; RPE, retinal pigment epithelium; OS, outer segment; IS, inner segment; ELM, external limiting membrane; ONL, outer-nuclear layer; OPL, outer plexiform layer; INL, inner nuclear layer; IPL, inner plexiform layer; GCL, glial cell layer. Magnification bar=2 µm.

and the INL. Morphologically, they represent displacement of the IS/OS material and the photoreceptor cell bodies into the inner retina due to the incomplete formation of the ELM and loss of the structural barrier [29]. The photoreceptor IS lose their orderly arrangement, and by 4 weeks of age, 25% of photoreceptors are short in the *rd8* mice when compared to WT mice [5]. A significant thinning of the IS and OS in the region with dysplasia was reported in *rd8* mice by 4 weeks of age. By 10 weeks, photoreceptor OS in *rd8* mice start to fragment resulting in the accumulation of granular debris in the sub-retinal space [5].

In contrast to the findings in the original colony of *rd8* mice, the $Wt^{rd8/rd8}$ and $Ctrp5^{+/-;\ rd8/rd8}$ mice in our L-ORD mouse colony did not show pseudorosette pathology even at 21 months of age, the oldest age tested in this study. The histology of the mice in the L-ORD colony was devoid of the characteristic features of the *rd8* phenotype. The $Wt^{rd8/rd8}$ and $Ctrp5^{+/-;\ rd8/rd8}$ mice showed well-defined nuclear layers (the INL and the ONL). The characteristic retinal changes that are prominent in *rd8* mice as early as 4 weeks were not observed in either the $Wt^{rd8/rd8}$ or $Ctrp5^{+/-;\ rd8/rd8}$ mice in our colony of L-ORD mice at least up to age 21 months.

The L-ORD mouse model develops AF lesions around 12 months with a subsequent progressive increase in the number of these lesions with age [20]. Contrary to the large number of AF lesions detected in $Ctrp5^{+/-;wt/wt}$ mice at older ages, a minimal number of spots were observed in the age-matched $Wt^{wt/wt}$ mice. Although AF lesions in 21-month-old $Ctrp5^{+/-;wt/wt}$ were distributed throughout the retina, the ocular spots observed in the *rd8* model were larger, heavily concentrated in the inferior quadrant of the fundus, and developed as early as 3 weeks of age. The *rd8* mice backcrossed onto the C57BL/6 background were reported to have a discontinuous ELM phenotype [5]. In contrast, the $Wt^{rd8/rd8}$ and $Ctrp5^{+/-;rd8/rd8}$ mice raised on the C57BL/6J background exhibited an uninterrupted outer limiting membrane. These observations indicate that the presence of the *Crb1* mutation in either the homozygous or heterozygous state failed to result in the development of the characteristic *rd8* phenotype in the $Wt^{rd8/rd8}$ and $Ctrp5^{+/-;\ rd8/rd8}$ mice in our L-ORD mouse colony. A review of retinal morphology and analysis of the genotype

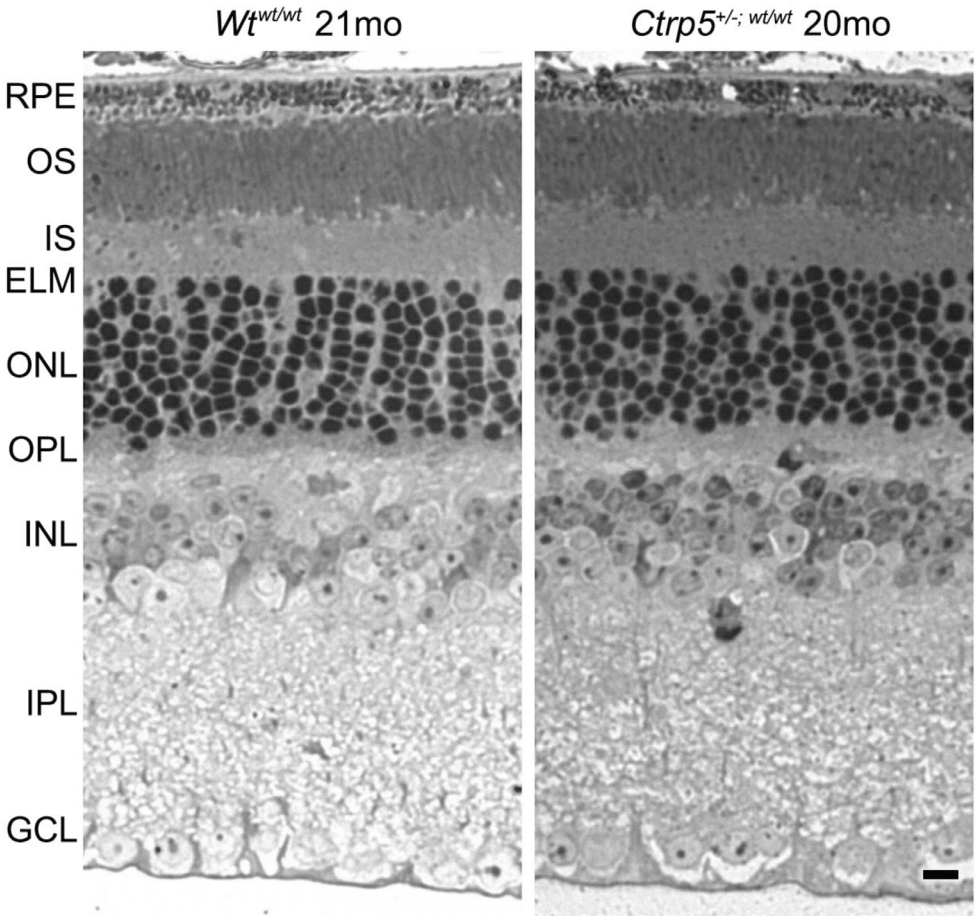

Figure 4. Histological analysis of the retinal structure of the L-ORD mice. Retinal changes typically associated with the *rd8* phenotype were not observed in either the $Ctrp5^{+/-;wt/wt}$ or $Wt^{wt/wt}$ mice at 20–21 months. In addition, the retinal morphology of these mice lacked gross abnormalities that can be detected with light microscopy. Magnification bar=20 µm.

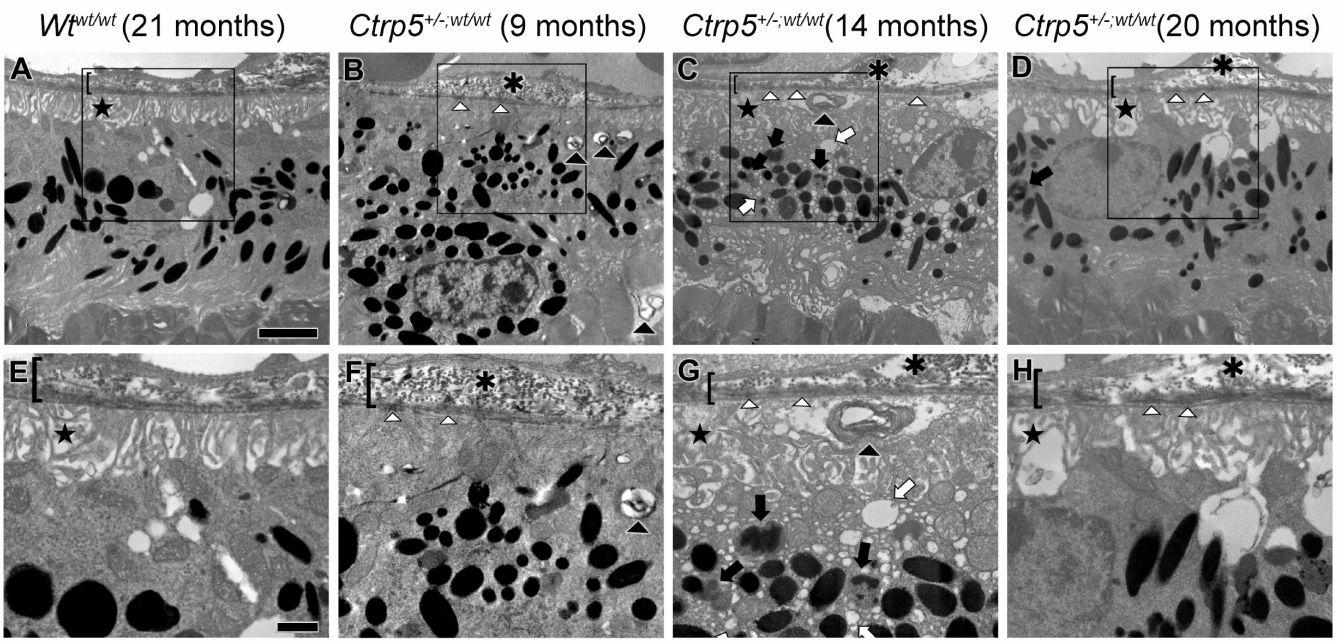

Figure 5. Ultrastructural analysis of RPE and sub-RPE areas from *Wt*$^{wt/wt}$ and Ctrp5$^{+/-;wt/wt}$ mice. Areas enclosed in boxes in **A**–**D** are magnified in panels **E**–**H**. RPE from control mice (**A**, **E**) showed no abnormalities at 21 months of age. The RPE basal infoldings are organized (star), the cytoplasm is homogenous, and Bruch's membrane is intact (bracket). In contrast, the RPE of the *Ctrp5*$^{+/-;wt/wt}$ mice (**B**, **C**, **D**, **F**, **G**, **H**) has structural aberrations beginning at 9 months of age. The RPE basal infoldings are disorganized (stars). Numerous packets of undigested membranous debris are found in the basal RPE (black arrowheads). Multiple vacuoles (white arrows) and phagolysosomes (black arrows) are found throughout the cytoplasm. Focal basal laminar deposits (white arrowheads) are present in Bruch's membrane, as are basal linear deposits (asterisks). All marking are identical to those used in all panels. Magnification bars=200 µm in the top row and 500 µm in the bottom row.

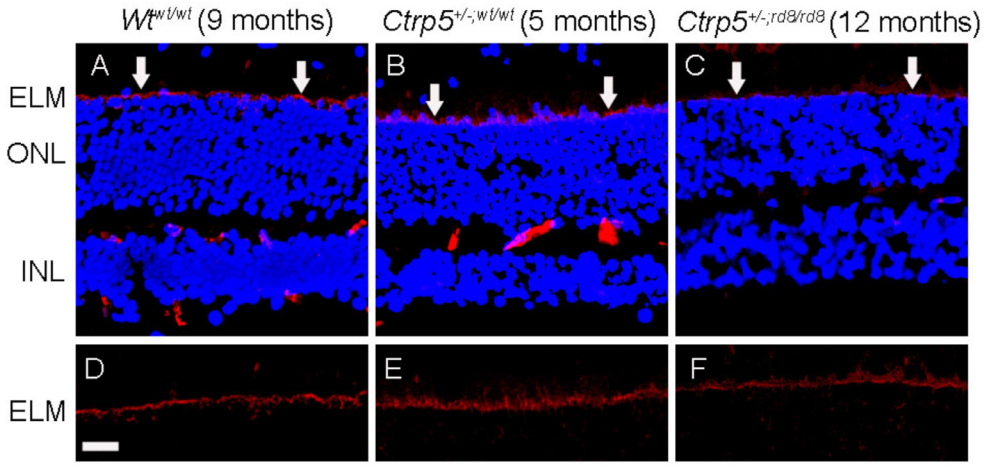

Figure 6. Continuous ELM staining with anti-adherence junction marker in L-ORD mice homozygous for the *rd8* mutation. **A**–**F** are stained with anti-β-catenin. **A**, **D**: Retinal specimen from *rd8* free wild-type control mouse (*Wt*$^{wt/wt}$) at 9 months of age. **B**, **E**: Retinal specimen from a 5-month-old late-onset retinal degeneration (L-ORD) mouse lacking the *rd8* mutation (*Ctrp5*$^{+/-;wt/wt}$). **C**, **F**: Retinal specimen from a 12-month-old L-ORD mouse homozygous for the *rd8* mutation (*Ctrp5*$^{+/-;rd8/rd8}$). Continuous staining is observed across the ELM in all genotypes. The arrows indicate the ELM. Magnification bar=4 µm. ELM, external limiting membrane, ONL, outer nuclear layer, INL, internal nuclear layer.

Table 2. Analysis of mice with L-ORD phenotype presented in Chavali et al. 2011.

Age (month)	Genotype (n=3)	Figures (Chavali et al. 2011)	Phenotype			
			Pseudo rosettes	Ocular lesion	Autofluorescent spots throughout retina	Number of cones
5	*Wt* $^{rd8/rd8}$	7A,9A	Absent	Absent	Absent	>200
	Ctrp5$^{+/-;\ rd8/rd8}$	7B,9B,9C	Absent	Absent	Absent	>200
8	*Wt* ND	6A,6B,7C,9D	Absent	Absent	Absent	>200
	Ctrp5$^{+/-;\ rd8/rd8}$	6A,6B,7D,9E, 9F	absent	Absent	3±1	>200
12	*Wt* ND	6A,6B,7E,9G,11	Absent	Absent	Absent	>200
	Ctrp5$^{+/-;\ rd8/rd8}$	6A,6B,7F,9H,9I,11	Absent	Absent	56±7	183±7
15	*Wt* $^{wt/rd8}$	6A,6B,7G,9J,11	Absent	Absent	15±5	>200
	Ctrp5$^{+/-;\ wt/rd8}$	6A,6B,7H,9K,9L,11	Absent	Absent	80±10	108±7
21	*Wt* ND	6A,6B,7I,9M,11	Absent	Absent	25±4	>200
	Ctrp5$^{+/-;\ wt/rd8}$	6A,6B,7J,9N,9O,11	Absent	Absent	>200	15±5

ND: not determined n=number of animals per assessment

of previously published L-ORD mice and wild-type controls revealed the absence of the *rd8*-associated phenotype at least up to 21 months [20].

In contrast to the findings in the L-ORD mice, the retinal pathology in the *rd8* model is clearly evident by 4 weeks with shortening and swelling of the IS and OS in *rd8* mice [5]. Abnormalities in the laminar architecture and retinal degeneration were also noted [5,29]. However, abnormal drusen-like, basal laminar, and basal linear deposits similar to those observed in the L-ORD mouse model were not reported in *rd8* mice [20]. The inferior retina of the *rd8* mouse is more severely affected with prominent dysplasia than the superior retina. These abnormalities were absent in the L-ORD mice even at 21 months [20]. These observations indicate that the presence of the *Crb1* mutation either in the heterozygous state or homozygous state did not result in the development of the *rd8* characteristic phenotype in the *Ctrp5*$^{+/-}$ mice in our L-ORD mouse colony.

The absence of the *rd8* retinal phenotype was noted not only in *Ctrp5*$^{+/-;\ rd8/rd8}$ mice but also in the littermate *Wt*$^{rd8/rd8}$ mice. This is consistent with the findings reported by Mehalow et al. for C57BL/6J mice [5]. In that study, a significant proportion of mice with a homozygous *Crb1* mutation on the C57BL/6J background did not exhibit *rd8*-associated retinal pathology, including ocular spots, retinal folds, pseudorosettes, inner segment shortening, and disorganization [5]. A more recent study by Luhman et al. reported that the homozygous *rd8* mutation on the C57BL/6 background leads to an increase in evenly distributed small discrete autofluorescent lesions on SLO fundus images [18].

It was hypothesized that the retinal abnormalities due to the *Crb1* mutation are strongly modulated by a genetic variant expressed in C57BL/6J mice [5]. Supporting this hypothesis, Luhmann et al. showed that an autosomal recessive locus in C57BL/6 can modulate the *rd8* phenotype in mice homozygous for the *Crb1* mutation [18,19]. The ES cells used to develop our L-ORD mice were a mixed population obtained from mice with C57BL/6J and C57BL/6N backgrounds. Subsequently, our L-ORD mice were bred with the C57BL/6J strain to maintain the mice line. It is likely that the modifier allele in the C57BL/6J strain is responsible for the absence of the *rd8* phenotype in our L-ORD mouse model colony.

The clinical phenotype of *Ctrp5*$^{+/-;rd8/rd8}$ and *Ctrp5*$^{+/-;wt/wt}$ mice is similar with characteristic late-onset sub-RPE deposits and Bruch's membrane abnormalities including basal laminar and basal linear deposits. This pathology is consistent with the phenotype observed in patients with L-ORD, while the retinal phenotype of age-matched *Wt*$^{wt/wt}$ and *Wt*$^{rd8/rd8}$ mice was normal. These observations clearly show that the presence of the *Crb1* mutation did not result in the development of retinal abnormalities in either *Ctrp5*$^{+/-;rd8/rd8}$ or littermate *Wt*$^{rd8/rd8}$ mice. In addition, these data demonstrate that the S163R mutation in *Ctrp5* in the heterozygous state leads to the development of the L-ORD phenotype and that the presence of *Crb1* mutation did not alter the retinal phenotype in these mice. It is likely that the presence of the *Crb1* mutation in addition to the *Ctrp5* mutation may result in additional changes that were not investigated in this study.

The autofluorescent spots reported by Luhman et al. in C57BL/6 mice with the *Crb1* mutation are similar to the

AF lesions observed in *Ctrp5*$^{+/-}$ mice [18]. It is possible that the AF lesions observed in *rd8*, *rd6*, *Ctrp5*, and chemokine-deficient mice with diverse genetic abnormalities may have a similar origin, and studying the pathobiology of these lesions may provide better understanding of the mechanism underlying RD.

Although this L-ORD mouse model (*Ctrp5*$^{+/-}$) generated on the C57BL/6J background developed late-onset retinal pathology, another knock-in model with the *Ctrp5* S163R mutation generated on the 129SV background (*Ctrp5*$^{+/-}$-129) did not develop retinal pathology even when older [30]. Shu et al. speculated that the genetic background may also influence the development of L-ORD pathology in mice [20,30]. Our current studies further support this hypothesis, and the identification of the underlying cause of variation in the phenotype between these two mouse models is likely to assist in understanding the molecular pathology of L-ORD and the development of therapeutic interventions to treat this condition.

ACKNOWLEDGMENTS

These studies were supported by: The Foundation Fighting Blindness, Thome Foundation in AMD Research, Research to Prevent Blindness (to Departments of Ophthalmology at UCSD, La Jolla, and University of Tennessee Health Science Center), R01EY13198, R01EY21237 and P30EY022589.

REFERENCES

1. Meuleman J, van de Pavert SA, Wijnholds J. Crumbs homologue 1 in polarity and blindness. Biochem Soc Trans 2004; 32:828-30. [PMID: 15494026].
2. van de Pavert SA, Kantardzhieva A, Malysheva A, Meuleman J, Versteeg I, Levelt C, Klooster J, Geiger S, Seeliger MW, Rashbass P, Le Bivic A, Wijnholds J. Crumbs homologue 1 is required for maintenance of photoreceptor cell polarization and adhesion during light exposure. J Cell Sci 2004; 117:4169-77. [PMID: 15316081].
3. Wodarz A, Hinz U, Engelbert M, Knust E. Expression of crumbs confers apical character on plasma membrane domains of ectodermal epithelia of Drosophila. Cell 1995; 82:67-76. [PMID: 7606787].
4. Jacobson SG, Cideciyan AV, Aleman TS, Pianta MJ, Sumaroka A, Schwartz SB, Smilko EE, Milam AH, Sheffield VC, Stone EM. Crumbs homolog 1 (CRB1) mutations result in a thick human retina with abnormal lamination. Hum Mol Genet 2003; 12:1073-8. [PMID: 12700176].
5. Mehalow AK, Kameya S, Smith RS, Hawes NL, Denegre JM, Young JA, Bechtold L, Haider NB, Tepass U, Heckenlively JR, Chang B, Naggert JK, Nishina PM. CRB1 is essential for external limiting membrane integrity and photoreceptor morphogenesis in the mammalian retina. Hum Mol Genet 2003; 12:2179-89. [PMID: 12915475].
6. den Hollander AI, Johnson K, de Kok YJ, Klebes A, Brunner HG, Knust E, Cremers FP. CRB1 has a cytoplasmic domain that is functionally conserved between human and Drosophila. Hum Mol Genet 2001; 10:2767-73. [PMID: 11734541].
7. Cremers FP, van den Hurk JA, den Hollander AI. Molecular genetics of Leber congenital amaurosis. Hum Mol Genet 2002; 11:1169-76. [PMID: 12015276].
8. den Hollander AI, Ghiani M, de Kok YJ, Wijnholds J, Ballabio A, Cremers FP, Broccoli V. Isolation of Crb1, a mouse homologue of Drosophila crumbs, and analysis of its expression pattern in eye and brain. Mech Dev 2002; 110:203-7. [PMID: 11744384].
9. Bernal S, Calaf M, Garcia-Hoyos M, Garcia-Sandoval B, Rosell J, Adan A, Ayuso C, Baiget M. Study of the involvement of the RGR, CRPB1, and CRB1 genes in the pathogenesis of autosomal recessive retinitis pigmentosa. J Med Genet 2003; 40:e89-[PMID: 12843338].
10. den Hollander AI, Davis J, van der Velde-Visser SD, Zonneveld MN, Pierrottet CO, Koenekoop RK, Kellner U, van den Born LI, Heckenlively JR, Hoyng CB, Handford PA, Roepman R, Cremers FP. CRB1 mutation spectrum in inherited retinal dystrophies. Hum Mutat 2004; 24:355-69. [PMID: 15459956].
11. den Hollander AI, Heckenlively JR, van den Born LI, de Kok YJ, van der Velde-Visser SD, Kellner U, Jurklies B, van Schooneveld MJ, Blankenagel A, Rohrschneider K, Wissinger B, Cruysberg JR, Deutman AF, Brunner HG, Apfelstedt-Sylla E, Hoyng CB, Cremers FP. Leber congenital amaurosis and retinitis pigmentosa with Coats-like exudative vasculopathy are associated with mutations in the crumbs homologue 1 (CRB1) gene. Am J Hum Genet 2001; 69:198-203. [PMID: 11389483].
12. den Hollander AI, ten Brink JB, de Kok YJ, van Soest S, van den Born LI, van Driel MA, van de Pol DJ, Payne AM, Bhattacharya SS, Kellner U, Hoyng CB, Westerveld A, Brunner HG, Bleeker-Wagemakers EM, Deutman AF, Heckenlively JR, Cremers FP, Bergen AA. Mutations in a human homologue of Drosophila crumbs cause retinitis pigmentosa (RP12). Nat Genet 1999; 23:217-21. [PMID: 10508521].
13. Lotery AJ, Jacobson SG, Fishman GA, Weleber RG, Fulton AB, Namperumalsamy P, Heon E, Levin AV, Grover S, Rosenow JR, Kopp KK, Sheffield VC, Stone EM. Mutations in the CRB1 gene cause Leber congenital amaurosis. Arch Ophthalmol 2001; 119:415-20. [PMID: 11231775].
14. Bujakowska K, Audo I, Mohand-Said S, Lancelot ME, Antonio A, Germain A, Leveillard T, Letexier M, Saraiva JP, Lonjou C, Carpentier W, Sahel JA, Bhattacharya SS, Zeitz C. CRB1 mutations in inherited retinal dystrophies. Hum Mutat 2012; 33:306-15. [PMID: 22065545].
15. Yzer S, Fishman GA, Racine J, Al-Zuhaibi S, Chakor H, Dorfman A, Szlyk J, Lachapelle P, van den Born LI, Allikmets R, Lopez I, Cremers FP, Koenekoop RK. CRB1

heterozygotes with regional retinal dysfunction: implications for genetic testing of leber congenital amaurosis. Invest Ophthalmol Vis Sci 2006; 47:3736-44. [PMID: 16936081].

16. Pang JJ, Chang B, Hawes NL, Hurd RE, Davisson MT, Li J, Noorwez SM, Malhotra R, McDowell JH, Kaushal S, Hauswirth WW, Nusinowitz S, Thompson DA, Heckenlively JR. Retinal degeneration 12 (rd12): a new, spontaneously arising mouse model for human Leber congenital amaurosis (LCA). Mol Vis 2005; 11:152-62. [PMID: 15765048].

17. Mattapallil MJ, Wawrousek EF, Chan CC, Zhao H, Roychoudhury J, Ferguson TA, Caspi RR. The Rd8 mutation of the Crb1 gene is present in vendor lines of C57BL/6N mice and embryonic stem cells, and confounds ocular induced mutant phenotypes. Invest Ophthalmol Vis Sci 2012; 53:2921-7. [PMID: 22447858].

18. Luhmann UF, Carvalho LS, Holthaus SM, Cowing JA, Greenaway S, Chu CJ, Herrmann P, Smith AJ, Munro PM, Potter P, Bainbridge JW, Ali RR. The severity of retinal pathology in homozygous Crb1rd8/rd8 mice is dependent on additional genetic factors. Hum Mol Genet 2015; 24:128-41. [PMID: 25147295].

19. Luhmann UF, Lange CA, Robbie S, Munro PM, Cowing JA, Armer HE, Luong V, Carvalho LS, MacLaren RE, Fitzke FW, Bainbridge JW, Ali RR. Differential modulation of retinal degeneration by Ccl2 and Cx3cr1 chemokine signalling. PLoS ONE 2012; 7:e35551-[PMID: 22545116].

20. Chavali VR, Khan NW, Cukras CA, Bartsch DU, Jablonski MM, Ayyagari RA. CTRP5 gene S163R mutation knock-in mouse model for late-onset retinal degeneration. Hum Mol Genet 2011; 20:2000-14. [PMID: 21349921].

21. Kuntz CA, Jacobson SG, Cideciyan AV, Li ZY, Stone EM, Possin D, Milam AH. Sub-retinal pigment epithelial deposits in a dominant late-onset retinal degeneration. Invest Ophthalmol Vis Sci 1996; 37:1772-82. [PMID: 8759344].

22. Milam AH, Curcio CA, Cideciyan AV, Saxena S, John SK, Kruth HS, Malek G, Heckenlively JR, Weleber RG, Jacobson SG. Dominant late-onset retinal degeneration with regional variation of sub-retinal pigment epithelium deposits, retinal function, and photoreceptor degeneration. Ophthalmology 2000; 107:2256-66. [PMID: 11097607].

23. Subrayan V, Morris B, Armbrecht AM, Wright AF, Dhillon B. Long anterior lens zonules in late-onset retinal degeneration (L-ORD). Am J Ophthalmol 2005; 140:1127-9. [PMID: 16376663].

24. Seeliger MW, Beck SC, Pereyra-Munoz N, Dangel S, Tsai JY, Luhmann UF, van de Pavert SA, Wijnholds J, Samardzija M, Wenzel A, Zrenner E, Narfstrom K, Fahl E, Tanimoto N, Acar N, Tonagel F. In vivo confocal imaging of the retina in animal models using scanning laser ophthalmoscopy. Vision Res 2005; 45:3512-9. [PMID: 16188288].

25. von Rückmann A, Fitzke FW, Bird AC. Distribution of fundus autofluorescence with a scanning laser ophthalmoscope. Br J Ophthalmol 1995; 79:407-12. [PMID: 7612549].

26. Koh HJ, Bessho K, Cheng L, Bartsch DU, Jones TR, Bergeron-Lynn G, Freeman WR. Inhibition of choroidal neovascularization in rats by the urokinase-derived peptide A6. Invest Ophthalmol Vis Sci 2004; 45:635-40. [PMID: 14744908].

27. Curcio CA, Rudolf M, Wang L. Histochemistry and lipid profiling combine for insights into aging and age-related maculopathy. Methods Mol Biol 2009; 580:267-81. [PMID: 19784605].

28. Jablonski MM, Tombran-Tink J, Mrazek DA, Iannaccone A. Pigment epithelium-derived factor supports normal development of photoreceptor neurons and opsin expression after retinal pigment epithelium removal. J Neurosci 2000; 20:7149-57. [PMID: 11007870].

29. Aleman TS, Cideciyan AV, Aguirre GK, Huang WC, Mullins CL, Roman AJ, Sumaroka A, Olivares MB, Tsai FF, Schwartz SB, Vandenberghe LH, Limberis MP, Stone EM, Bell P, Wilson JM, Jacobson SG. Human CRB1-associated retinal degeneration: comparison with the rd8 Crb1-mutant mouse model. Invest Ophthalmol Vis Sci 2011; 52:6898-910. [PMID: 21757580].

30. Shu X, Luhmann UF, Aleman TS, Barker SE, Lennon A, Tulloch B, Chen M, Xu H, Jacobson SG, Ali R, Wright AF. Characterisation of a C1qtnf5 Ser163Arg knock-in mouse model of late-onset retinal macular degeneration. PLoS ONE 2011; 6:e27433-[PMID: 22110650].

Articles are provided courtesy of Emory University and the Zhongshan Ophthalmic Center, Sun Yat-sen University, P.R. China. The print version of this article was created on 13 March 2015. This reflects all typographical corrections and errata to the article through that date. Details of any changes may be found in the online version of the article.